Applied Catalysis B: Environmental 150–151 (2014) 612–618

Contents lists available at ScienceDirect

Applied Catalysis B: Environmental

journal homepage: www.elsevier.com/locate/apcatb

The constraints of transition metal substitutions (Ti, Cr, Mn, Co and Ni) in magnetite on its catalytic activity in heterogeneous Fenton and UV/Fenton reaction: From the perspective of hydroxyl radical generation

Yuanhong Zhong[a,b], Xiaoliang Liang[a], Zisen He[a,b], Wei Tan[a,b], Jianxi Zhu[a], Peng Yuan[a], Runliang Zhu[a], Hongping He[a,*]

[a] Key Laboratory of Mineralogy and Metallogeny, Guangzhou Institute of Geochemistry, Chinese Academy of Sciences, Guangzhou 510640, China
[b] University of Chinese Academy of Sciences, Beijing 100049, China

ARTICLE INFO

Article history:
Received 10 September 2013
Received in revised form 2 January 2014
Accepted 4 January 2014
Available online 13 January 2014

Keywords:
Magnetite
Hydroxyl radicals
Isomorphous substitution
Heterogeneous Fenton
UV/Fenton

ABSTRACT

In this paper, the heterogeneous Fenton and UV/Fenton catalytic activities of transition metal substituted magnetites, $Fe_{3-x}M_xO_4$ (M = Ti, Cr, Mn, Co and Ni), were compared in the perspective of •OH radicals generation. In heterogeneous Fenton reaction, the substitutions of Cr(III), Mn(II) and Co(II) enhanced the rate of •OH formation, while Ni(II) and Ti(VI) showed the negative effect. In heterogeneous UV/Fenton reaction, the Ni(II) and Co(II) introduction did not show notable changes on •OH generation efficiency, whetreas the Cr(III), Ti(VI) and Mn(II) incorporation improved this reaction and accordingly enhanced the UV/Fenton catalytic activity of magnetite. Redundancy and Pearson correlation analyses were carried out to interpret the influence factors in Fenton and UV/Fenton reactions.

1. Introduction

Increasing attention has been paid to heterogeneous Fenton-like reaction, due to its potential effectiveness in the mineralization of organic pollutants in a wide range of reaction pH, and limited iron leaching for catalyst recycle [1–3]. Recent studies showed that aqueous hydrogen peroxide can be decomposed over various solid catalysts, e.g., zeolite-supported iron [4,5], iron pillared interlayered clays [6,7], and iron oxide minerals (goethite, hematite, magnetite, and ferrihydrite), [8,9] via the Haber–Weiss mechanism (Eq. (1)) to form highly reactive and non-selective hydroxyl radicals (•OH). With a quite high redox potential (2.80 eV), •OH radicals can oxidize and mineralize most organic substances in environment [10–12]. Previous studies have shown that •OH production is a critical factor affecting the degradation efficiency of contaminants in various water treatment techniques [1,13–16]. Therefore, it is significant to examine the generation rate of •OH radicals for testing the catalytic activity of various Fenton-like catalysts.

$$\equiv Fe(II) + H_2O_2 \rightarrow \equiv Fe(III) + {}^{\bullet}OH + OH^- \quad (1)$$

Magnetite (Fe_3O_4) is an efficient Fenton catalyst among the iron oxide minerals [2,17], possibly because it accommodates both Fe(II) and Fe(III) in the structure and can be reversibly oxidized and reduced while the same structure is remained. Moreover, magnetite is a magnetic mineral and can be easily recycled in the practical wastewater decontamination. As a ubiquitous mineral on the earth surface system (e.g., soil, sediments and various weathered products), magnetite is not only a promising mineral in the pollution remediation, but also closely linked to the fate of contaminants in the nature. In natural magnetite, iron cations are usually isomorphically substituted by divalent (Co, Ni, Zn, Cu, Mn, etc.), trivalent (Al, V, Cr, etc.) and tetravalent (Ti) cations while maintaining the spinel structure [18]. As indicated by previous researches [10,11,19–21], some substitutions obviously varied the catalytic activity of magnetite in heterogeneous Fenton reaction. The introduction of Mn^{2+} [10,11], Co^{2+} [10,11], V^{3+} [22], Ti^{4+} [21] and Cr^{3+} [12,19] improved the catalytic activity of magnetite in the degradation of organic pollutants (e.g., methylene blue, phenol and acid orange II), while Ni^{2+} showed an inhibitory effect [11]. These variations relied on two aspects, i.e., the generation rate of •OH radicals and adsorption ability of organic pollutants and H_2O_2 onto magnetite surface. Some substitutions improved the surface properties of magnetite, such as specific surface area and superficial hydroxyl amount. These variations enhanced the adsorption of

* Corresponding author. Tel.: +86 20 85290257; fax: +86 20 85290130.
E-mail address: hehp@gig.ac.cn (H. He).

0926-3373/$ – see front matter © 2014 Elsevier B.V. All rights reserved.
http://dx.doi.org/10.1016/j.apcatb.2014.01.007

organic pollutants and H_2O_2 on magnetite surface and accordingly accelerated the degradation process [19,20]. Therefore, to illustrate the improvement mechanism of substitutions on the catalytic activity of magnetite, it is important to distinguish the contributions from these two aspects on the degradation enhancement. To the best of our knowledge, the effect of substitutions on the adsorption properties of magnetite has been widely investigated through batch adsorption experiment, but few studies have been carried out to explore the •OH radicals generation process and the contribution of the potential influencing factors in this kind of Fenton system. Petigara et al. [15] examined the •OH formation rate in a series of soil suspensions and concluded that •OH was a major product of H_2O_2 decomposition in soils with low organic matter content, but was a minor product in soils with high organic matter or manganese content. Kwan et al. [16] found that different iron oxides displayed different rates of •OH production ($V^{\bullet}_{OH}$), and $V^{\bullet}_{OH}$ was proportional to the product-term of H_2O_2 concentration and the surface area of iron oxides. Unfortunately, they did not consider the other important factors, e.g., the heterogeneity of crystalline structure, adsorption process and the impurities in iron oxides. These studies illustrated the diversity in the yield of •OH radicals by iron oxides, so a more comprehensive study on the role of •OH generation in heterogeneous Fenton reaction is imperative, especially for iron oxides with homologous isomorphous substitution.

It has been widely acknowledged that Fenton reaction rates are usually greatly increased in the presence of UV light. Hence the influence of substitutions on the heterogeneous UV/Fenton activity of magnetite also has been investigated [22–24]. The Ti^{4+} incorporation in magnetite obviously enhanced its UV/Fenton activity in the degradation of tetrabromobisphenol A (TBBPA) [24]. The distinct effect of substitutions were proved in the order of Co < Mn < Ti ≈ Ni < Cr [23], which were ascribed to the enhancement of both •OH radicals generation and adsorption properties. Similar to the Fenton system, the effect of substitutions on the •OH generation in heterogeneous UV/Fenton system has not been evaluated. Since •OH is the main active radical in Fenton reaction, it is necessary to determine their generation rate and concentration during the reaction.

In the current study, the yield rate and concentration of •OH radicals were analyzed in the heterogeneous Fenton and UV/Fenton systems catalyzed by various metal (Ti, Cr, Mn, Co and Ni) substituted magnetites. The mechanism about different effects of substitutions on the •OH radicals generation and the relationship between •OH radicals generation and the catalytic performance in the organic pollutant degradation were discussed. The multivariate analyses were also performed to distinguish the major and minor factors affecting the Fenton and UV/Fenton progress. The obtained results are of high importance for better understanding the effect of transition metal substitutions on the catalytic activity of magnetite towards Fenton and UV/Fenton reactions.

2. Experimental

2.1. Preparation and characterization of magnetite samples

The substituted magnetite samples were synthesized by a precipitation-oxidation method as described in our previous publications [21,24]. From chemical analysis, the chemical formulae of magnetite samples were Fe_3O_4, $Fe_{2.02}Ti_{0.98}O_4$, $Fe_{2.04}Cr_{0.96}O_4$, $Fe_{2.15}Mn_{0.85}O_4$, $Fe_{2.19}Co_{0.91}O_4$ and Fe_2NiO_4, labeled as M, Ti–M, Cr–M, Mn–M, Co–M and Ni–M, respectively. The molar ratio between iron and substituting metal was almost 2:1, suggesting that these samples were on similar substitution level. The characterization of X-ray diffraction (XRD, Fig. A.1) showed that all the magnetite samples had spinel structure, but in Ni–M and Mn–M, iron chloride hydroxide and feitknechtite were found in quite low content, respectively. The X-ray absorption near edge structure (XANES) results illustrated that the substituting cations have entered the spinel structure. Ti(VI), Cr(III), Mn(III), Co(II), and Ni(II) mainly occupied the octahedral sites of spinel structure while Mn(II) occupied the tetrahedral ones. The detailed discussion of XANES results has been presented elsewhere [23,25]. The main physical and chemical properties (i.e., lattice constants a_0, BET specific surface area, average crystal size, surface hydroxyl amount, pH_{pzc} and saturation isothermal remanence) of the magnetite samples were also analyzed (Text A.1) and the results are displayed in Table A.1 in Supplementary material.

2.2. •OH radicals production test

•OH radicals generated in heterogeneous Fenton and UV/Fenton processes were trapped with dimethyl sulfoxide (DMSO) to produce formaldehyde quantitatively [14,26,27], then reacted with 2,4-dinitrophenylhydrazine (DNPH) to form hydrazone (DNPHo) and were analyzed by high performance liquid chromatography (HPLC) [28]. The details of analysis procedure are provided in Text A.2 in Supplementary material. The tests were conducted in triplicate.

2.3. Degradation of p-nitrophenol (PNP) and tetrabromobisphenol A (TBBPA)

The degradation of persistent organic pollutants (POPs) PNP and TBBPA was conducted to illustrate the effect of •OH generation on the degradation of organic pollutants. The PNP concentration was determined by UV–Vis spectrophotometer (PerkinElmer Lambda 850), while TBBPA was analyzed by HPLC [24]. The details of degradation experiment procedure are described in Text A.3 in Supplementary material. The degradation experiment was conducted in triplicate.

2.4. Data analysis

The redundancy analysis (RDA) is similar to principal component analysis (PCA), but using linear combinations to constrain the main axes of environmental variables [29,30]. In this study, RDA was used to determine which of the measured properties of magnetite samples (explanatory variables) dominated the variation in the degradation efficiency (response variable), in order to distinguish the major and minor factors. RDA was executed by using CANOCO for Windows package, version 4.5 (Ter Braak & Smilauer, Wageningen, the Netherlands). The degradation efficiency in Fenton and UV/Fenton systems catalyzed by substituted magnetites were expressed as efficiency response variables. The physicochemical properties of magnetites, including BET specific surface area, surface hydroxyl amount, pH_{pzc} (the pH of point of zero charge), lattice constant a_0, average crystal size, ionic radius of substitution cations, saturation isothermal remanence (SIRM), adsorption property and generated •OH radicals concentration were determined as potential influence variables data. These data were log $(x+1)$ transformed. Then the detrended correspondence analysis (DCA) of the efficiency variance was performed to detect the length of the ordination gradient which determined the underlying distribution pattern of data. RDA was performed as the length of the gradient along the first axe was 0.299 (<3.0), thus the linear response model was chosen to test for normality of the explanatory variables. Then it was followed by Monte Carlo permutation tests with 499 permutations and unrestricted permutations under a reduced model, to test which explanatory variables were dominant.

Pearson correlation analysis was calculated to further assess the associations among all the assigned variables. The linear regression

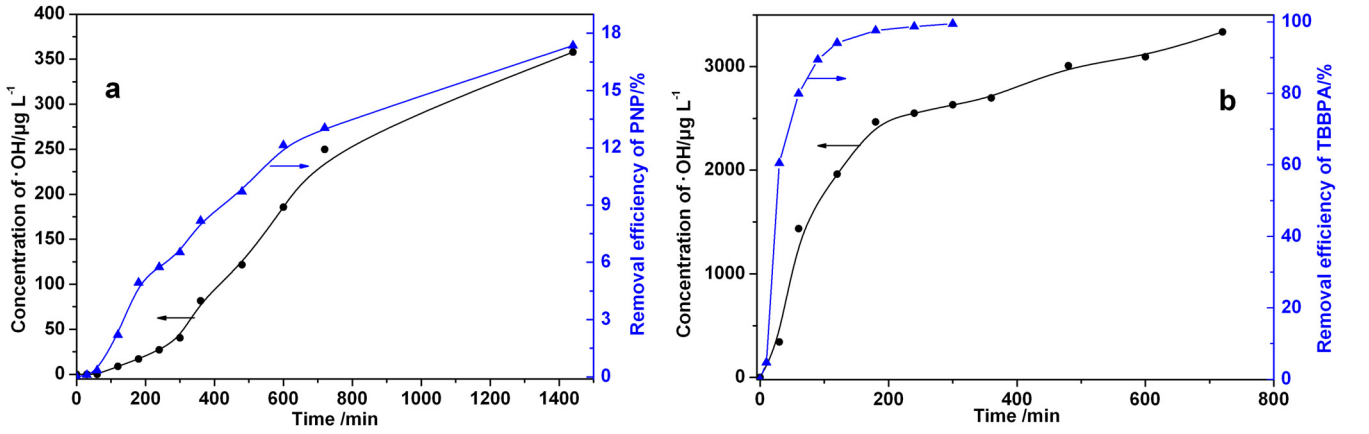

Fig. 1. The effect of •OH radicals generation process on the degradation of PNP in heterogeneous Fenton reaction (a) and TBBPA in heterogeneous UV/Fenton reaction (b) (catalyst: 0.5 g L^{-1}, H_2O_2: 10 mmol L^{-1}, PNP: 10 mg L^{-1}, TBBPA: 20 mg L^{-1}).

function analysis was conducted in SPSS V13.0, and performed by applying the stepwise selection procedures.

3. Results and discussion

3.1. •OH generation in heterogeneous Fenton system

To investigate the role of •OH generation in the degradation of organic pollutants, two different POPs, PNP and TBBPA, were chosen as the model pollutants in heterogeneous Fenton and UV/Fenton reactions catalyzed by Cr–M, respectively. With the presence of excess H_2O_2, H_2O_2 would be decomposed to water and oxygen via non-radical pathways [15,16]. So relatively low concentration of H_2O_2 (10 mM) was employed in our experiments and little O_2 production was obtained. In both Fenton and UV/Fenton systems, the •OH concentration increased with the reaction proceeded, implying that the Fenton reaction was mainly through the hydroxyl radical-mediated mechanism. The kinetic curves of PNP (Fig. 1a) and TBBPA (Fig. 1b) degradation were quite identical to those of •OH generation, indicating that •OH should be the main active radicals in heterogeneous Fenton and UV/Fenton degradation [1,31]. Therefore, it is significant to evaluate the contribution of •OH generation to the catalytic performance of magnetite samples.

To compare the Fenton catalytic activity of magnetites substituted by different transition metals, the •OH radicals generation was traced in the Fenton systems with synthetic magnetites (Fig. 2).

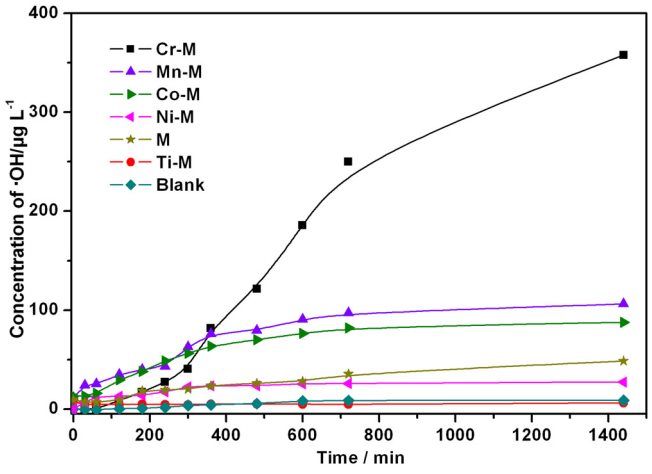

Fig. 2. The kinetics of •OH radicals generation in the heterogeneous Fenton systems catalyzed by magnetites.

The kinetic process of •OH generation was divided into two stages with different rates. The average generation rates of •OH radicals ($V^{\bullet}_{OH}$) were listed in Table 1. In the blank system with H_2O_2 alone, •OH radicals were hardly detected in 24 h. But after the addition of magnetite M, •OH concentration obviously increased, reflecting the Fenton catalytic activity of magnetite. For the systems with Cr–M, Mn–M and Co–M, more •OH radicals were produced than the system with M. Especially for the system with Cr–M, which showed the most intense •OH generation, the average $V^{\bullet}_{OH}$ in 24 h was up to 0.25 μg L^{-1} min^{-1}, about eight times higher than that the system with M (0.03 μg L^{-1} min^{-1}). From previous researches [10–12,19], the presence of Co, Mn and Cr in magnetite structure engendered a remarkable increase of Fenton reactivity of magnetite towards the degradation of methylene blue. In this study, these substitutions obviously improved the activity of magnetite in •OH generation, which can well explain their positive effect on the Fenton activity of magnetite. Contrary to Cr–M, Mn–M and Co–M, the systems with Ni–M and Ti–M produced quite few •OH radicals. The average generation rate for 24 h in Ni–M system (0.02 μg L^{-1} min^{-1}) was lower than that of M (0.03 μg L^{-1} min^{-1}), indicating that Ni showed an inhibitive effect on the Fenton catalytic activity of magnetite. The negative effect of Ni(II) was also found in the study by Costa et al. [11], where Ni^{2+} inhibited the H_2O_2 decomposition and the reaction rate decreased as Ni content increased. The restraining effect of Ti(VI) incorporation was more obvious than Ni(II), as the •OH generation process by titanomagnetite was quite identical to that of blank system and almost no •OH radicals was produced. This result supported our previous conclusion that Ti in $Fe_{3-x}Ti_xO_4$ may not participate in the heterogeneous Fenton reaction through hydroxyl radical mediated mechanism. The improvement of methylene blue degradation by Ti incorporation mainly depended on the enhanced adsorption on the titanomagnetite surface [21]. To explain the

Table 1
The average generation rate of •OH radicals ($V^{\bullet}_{OH}$) in the heterogeneous Fenton systems.

Catalyst	In the first 2 h (μg L^{-1} min^{-1})	From 2 to 12 h (μg L^{-1} min^{-1})	In total 24 h (μg L^{-1} min^{-1})
Cr-M	0.07	0.40	0.25
Mn-M	0.29	0.10	0.07
Co-M	0.25	0.09	0.06
Ni-M	0.11	0.02	0.02
M	0.07	0.03	0.03
Ti-M	0	0	0
Blank	0	0	0

$V^{\bullet}_{OH}$: The total amount of generated •OH divided by reaction time.

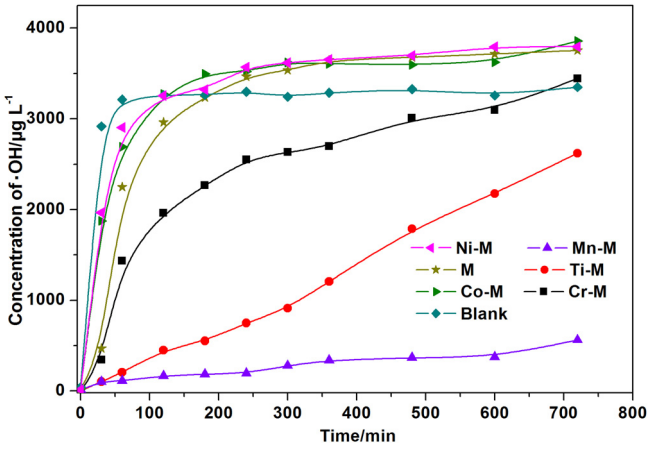

Fig. 3. The kinetics of •OH radicals generation in the heterogeneous UV/Fenton systems catalyzed by magnetites.

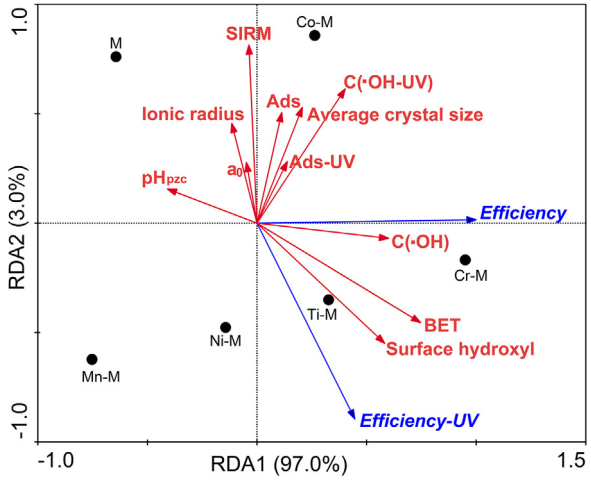

Fig. 4. RDA ordination biplot based on the degradation efficiency of the organic substance and the potential contributing of physicochemistry properties variables from the isomorphous replacement (Ads and Ads-UV: adsorption of PNP in Fenton and TBBPA in UV/Fenton system, C(•OH) and C(•OH-UV): the concentration of generated •OH radicals at the setting experiment time in Fenton and UV/Fenton systems).

different effects of these substitutions on •*OH* production, their distinct redox properties should be considered. For Cr(III), Mn(II) and Co(II), they exhibited the redox pairs Cr(II)/Cr(III), Mn(II)/Mn(III) and Co(II)/Co(III). So they produced •OH radicals through the H_2O_2 decomposition and accelerated the electron transfer in the magnetite structure during the reaction. But for Ti and Ni, only Ti(VI) and Ni(II) were stable species, and could not initiate the reaction.

3.2. •*OH formation in heterogeneous UV/Fenton system*

The •OH formation process catalyzed by the magnetites were also investigated under UV irradiation. After the introduction of UV light, the •OH formation was significantly enhanced (Fig. 3). The positive effect of UV light on the improvement of •OH generation was ascribed to the iron recycling caused by the photochemical reduction of ferric ions, and accordingly promoted the Fenton reaction [32]. The kinetic process of •OH generation also could be divided into two stages (Table 2). In the blank system, the average $V^{\bullet}_{OH}$ was up to 53.54 μg L^{-1} min^{-1} in the initial 60 min, but dropped sharply due to the fast depletion of H_2O_2 by UV radiation (Eq. (2)).

$$H_2O_2 + h\nu \rightarrow 2^{\bullet}OH \quad (2)$$

In the UV/Fenton systems catalyzed by synthetic magnetites, the yield rates of •OH radicals in the first hour were lower than that of blank system, ascribed to the shielding effect from the black catalyst particles suspending in the solution. But with the reaction proceeding, the generation rate became higher than that in the blank system, indicating the catalytic role of magnetites. Within the studied reaction time, three systems catalyzed by M, Ni–M and Co–M generated more •OH radicals than the blank system. But the produced amount of •OH radicals in the systems containing Ni–M and Co–M was close to that in the system with M, suggesting that

Table 2
The average generation rate of •OH radicals ($V^{\bullet}_{OH}$) in the heterogeneous UV/Fenton systems.

Catalyst	In the first 1 h (μg L^{-1} min^{-1})	From 1 to 12 h (μg L^{-1} min^{-1})	In total 12 h (μg L^{-1} min^{-1})
Cr–M	23.94	2.82	4.58
Ti–M	3.44	3.66	3.64
Ni–M	48.39	1.35	5.27
Mn–M	1.87	0.68	0.78
Co–M	44.87	1.77	5.36
M	37.48	2.28	5.21
Blank	53.54	0.21	4.65

Ni and Co did not show notable effects on the •OH generation efficiency. This further implied that the improvement of Ni and Co substitution on the UV/Fenton catalytic performance of magnetite in TBBPA degradation mainly depended on the enhanced absorption (Fig. A.2), due to the increase of BET specific surface area and surface hydroxyl amount (Fig. A.3). For the other three systems catalyzed by Cr–M, Ti–M and Mn–M, the production amount of •OH was obviously low at the beginning of reaction, but later increased continuously. The •OH concentration in Ti–M and Mn–M containing systems increased with an approximate linear relationship, but the generation rate in the system with Ti–M was much higher than that with Mn–M. Although the •OH generation was inhibited by Ti(IV) substitution in Fenton system, under the UV irradiation the Ti(IV) on Ti–M surface was reduced to Ti(III) and simultaneity produced oxygen vacancies, which provided more active sites to produce •OH [24,33,34]. For Cr–M containing system, its initial rate was lower than that in the system with M, but the average rate in 1–12 h was 2.82 μg L^{-1} min^{-1}, which was higher than the other systems except that with Ti–M. From the above observations, the UV/Fenton catalytic system with faster •OH generation (e.g., M, Co–M and Ni–M), had lower efficiency in TBBPA degradation, which was probably ascribed to the fact that the excessive •OH generated in a short time would be quenched by H_2O_2 to form weaker oxidative perhydroxyl radicals ($HO_2^{\bullet}$) as expressed in Eq. (3) [35,36], leading to less effective degradation.

$$^{\bullet}OH + H_2O_2 \rightarrow HO_2^{\bullet} + H_2O \quad (3)$$

From the trend of •OH generation by Cr–M, Ti–M and Mn–M (Fig. 3), the yield amount of •OH increased sustainably as the reaction continued. Therefore, their excellent catalytic activity in TBBPA degradation [23] was possibly related to not only the increased surface properties (Fig. A.3), but also the continuous generation of •OH radicals. A more comprehensive study is needed to determine the dominant factors of the catalytic performance of magnetite samples.

3.3. *Redundancy analysis*

Data from both Fenton and UV/Fenton reactions catalyzed by substituted magnetites were analyzed to assess the effects of •OH concentration and other potential explanatory variables on the removal efficiency. In the ordination diagrams (Fig. 4), six

substituted magnetite samples data are indicated with black circles. The length of arrows indicates the relationship strength between the explanatory variable and the response variable. The intersection angles between two arrows (cosine value) express the correlation among the variables. Moreover, the distance between the sample points exhibits the dissimilarity among the representative samples [29]. RDA results shows that 97.0% of the remaining variance is captured in the first axes, and this means that 97.0% of the response variables in the data set are explained by the measured explanatory variables. The ordination biplot displays that three influence variables (i.e., C(•OH), BET specific surface area and surface hydroxyl amount) are positively correlated with RDA axis 1, and positively correlated with the *Efficiency* and *Efficiency-UV*. Contrarily, the other four influence variables (SIRM, a_0, ionic radius and pH_{pzc}) are negatively correlated with the *Efficiency*, as their intersection angles are greater than 90°. The minimum intersection angle is found between the *Efficiency* and C(•OH), suggesting that the removal efficiency of magnetites in Fenton reaction was mainly dependent on the •OH concentration, subsequently influenced by BET specific surface area and surface hydroxyl amount. As shown in Fig. 4, the sample Cr–M is the closest to C(•OH). This indicates that the highest removal efficiency in Fenton system catalyzed by Cr–M is due to the highest •OH concentration of generated radicals. For Ti–M, its reactivity is dependent on the enlarged superficial hydroxyl groups and BET specific surface area rather than the concentration of •OH radicals, while that of Co–M is more correlated with its strong adsorption property. These results are consistent with the observations in above •OH formation. However, no exclusive influence factor is noticed in system catalyzed by Mn–M and Ni–M samples. The possible explanation is that RDA cannot always make accurate interpretations, especially for Ni–M and Mn–M with impurity phases.

When it comes to UV/Fenton system, it can be observed that the *Efficiency-UV* was mainly determined by the surface hydroxyl amount, and secondly affected by BET specific surface area (Fig. 4). Thus the substituted magnetites with stronger catalytic activity for TBBPA degradation are mainly ascribed to the enhanced specific surface area and surface hydroxyl amount (Fig. A.3). Taking Co–M for example, although its BET specific surface area is twice lower than that of M, the degradation efficiency still increases. This is due to the fact that its surface hydroxyl amount is over triple higher than that of M (Table A.1). The C(•OH-UV) is also an important factor and cannot be ignored. It is negatively correlated with the *Efficiency-UV* and shows a longish arrow. This means that a rapid rate of •OH generation probably inhibits the UV/Fenton efficiency, while a suitable generated rate of •OH would be beneficial for the degradation. It is possible that as the UV light is introduced into the Fenton system, the removal behavior of contaminants catalyzed by magnetites becomes complicated, where the mechanism involves a multiple sinks of H_2O_2 and •OH. The short arrow of the Ads-UV implies that it contributes less to the explanation of the *Efficiency-UV* variation. From the distance between the substituted sample points and M point, it can be predicted that the substitution of transition metals improves the heterogeneous UV/Fenton degradation efficiency. Among these substituted samples, Cr–M has the strongest catalytic activity for degradation of organic compounds while Co–M is the weakest. These important correlations summarized from this diagram are consistent with our previous conclusions that the substituted cations improve the heterogeneous UV/Fenton efficiency of magnetites as the order of Co < Mn < Ti ≈ Ni < Cr [23].

The correlation matrix of all assigned variables by Pearson correlation analysis at the 95% confidence level ($P < 0.05$) is shown in Table 3. The correlation coefficient further reveals that the degradation efficiency of Fenton system has a significant relation with C(•OH), BET specific surface area and surface hydroxyl amount,

Table 3
The correlation matrix of all assigned variables by Pearson correlation analysis at the 95% confidence level ($P < 0.05$).

	ACS[a]	a_0	BET[b]	SH[c]	Ionic radius	pH_{pzc}	SIRM[d]	C(•OH)*	Adsorption*	Efficiency*	C(•OH)	Adsorption	Efficiency
ACS[a]	1.000												
a_0	0.752	1.000											
BET[b]	–	–	1.000										
SH[c]	–	–	0.823	1.000									
Ionic radius	0.808	0.983	–	–	1.000								
pH_{pzc}	0.695	0.972	–	–	0.983	1.000							
SIRM[d]	0.830	–	–	–	–	–	1.000						
C(•OH)*	–	–	–	–	–	–	–	1.000					
Adsorption*	0.701	–	–	–	–	–	0.716	–	1.000				
Efficiency*	–	–	0.807	0.809	–	–	–	–	–	1.000			
C(•OH)	–	–	0.726	–	–	–	–	–	–	–	1.000		
Adsorption	0.793	–	–	–	–	–	0.797	–	0.881	–	–	1.000	
Efficiency	–	–	0.856	0.629	–	–	–	–	–	–	0.794	–	1.000

Data do not show in this table owing to no significant correlation with each other ($P > 0.05$ and $R^2 < 0.50$).

[a] Average crystal size.
[b] BET specific surface area.
[c] Surface hydroxyl amount.
[d] Saturation isothermal remanence.
* The variables in UV/Fenton system.

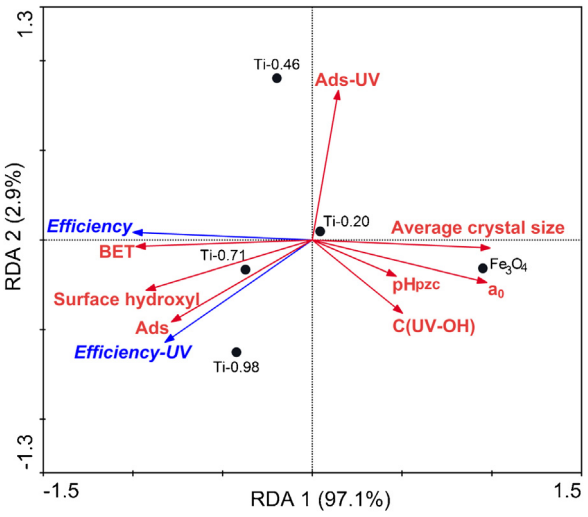

Fig. 5. RDA ordination biplot based on the degradation efficiency of the organic substance catalyzed by titanomagnetite ($Fe_{3-x}Ti_xO_4$, $x \leq 1.0$) and the potential contributing of physicochemistry properties variables from titanium replacement (Ads and Ads-UV: adsorption of methylene blue in Fenton and TBBPA in UV/Fenton system).

while UV/Fenton are mainly dependent on the latter two variables. It is also exhibited that the connection among the other variables, i.e., a_0, ionic radius, pH_{pzc}, average crystal size and SIRM, mainly affect the adsorption behavior instead of degradation.

In the above analysis on the relationship between the properties of magnetites and their catalytic performance, the property values used was deduced from magnetites with substitutions by different metal cations. To exclude the influence of metal species on the resultant relationship, redundancy analyses (Fig. 5) were also performed on the magnetites with different substitution extent by the same cation. The physical and chemical parameters of Ti substituted magnetites ($Fe_{3-x}Ti_xO_4$, $x = 0, 0.20, 0.46, 0.71, 0.98$) are shown in Table A.2. Due to the fact that almost no •OH radicals was produced in the Fenton reaction catalyzed by $Fe_{3-x}Ti_xO_4$, the influence of •OH generation on the Fenton efficiency was ignored. In Fig. 5, the intersection angles indicate that the Fenton *Efficiency* and *Efficiency-UV* of $Fe_{3-x}Ti_xO_4$ are mainly dependent on BET surface area and surface hydroxyl amount. But these two properties contribute more to the Fenton efficiency than to the UV/Fenton efficiency. Obviously, the adsorption is beneficial to improve degradation in Fenton system, but it contributes less to the degradation in UV/Fenton system. The C(•OH-UV) is not the dominant factor in UV/Fenton system, but it cannot be ignored. The variables of a_0, pH_{pzc} and average crystal size show lower influence on the *Efficiency* and *Efficiency-UV*. These conclusions are well consistent with those from the previous discussion based on the magnetites doped with different cations.

4. Conclusion

In the present study, •OH generation in the heterogeneous Fenton and UV/Fenton systems catalyzed by transition metal substituted magnetites $Fe_{3-x}M_xO_4$ (M = Ti, Cr, Mn, Co and Ni) was investigated. Cr(III), Mn(II) and Co(II) improve the •OH generation rate and accordingly enhance the Fenton catalytic activity of magnetite, while Ni(II) and Ti(IV) show a negative effect. Cr substituted magnetite displays the highest rate of •OH generation in Fenton system. In heterogeneous UV/Fenton system, Ni(II) and Co(II) do not show notable effects on the •OH generation efficiency. The Cr(III), Ti(IV) and Mn(II) effectively inhibit the fast decomposition of H_2O_2 and improve the •OH generation, which accordingly improve the catalytic capability of magnetite. RDA and Pearson correlation analyses show that the degradation efficiency of Fenton system has a close relationship with the concentration of •OH, BET specific surface area and surface hydroxyl amount, while UV/Fenton are mainly dependent on the latter two variables. By contrast, the adsorption fractions contribute less to the explanation of the efficiency variation. These results are helpful in understanding the effect of the transition metal substitution on the Fenton and UV/Fenton catalytic activity of magnetite and the critical factors that control the degradation efficiency of organic compounds catalyzed by magnetite.

Acknowledgments

This is contribution No. IS-1803 from GIG CAS. We gratefully acknowledge the financial support provided by the National Natural Science Foundation of China (Grant No. 41172045) and Guangzhou Institute of Geochemistry, Chinese Academy of Sciences (GIGCAS 135 project Y234041001).

Appendix A. Supplementary data

Supplementary data associated with this article can be found, in the online version, at http://dx.doi.org/10.1016/j.apcatb.2014.01.007.

References

[1] E.G. Garrido-Ramirez, B.K.G. Theng, M.L. Mora, Appl. Clay Sci. 47 (2010) 182–192.
[2] M.C. Pereira, L.C.A. Oliveira, E. Murad, Clay Miner. 47 (2012) 285–302.
[3] J.H. Deng, J.Y. Jiang, Y.Y. Zhang, X.P. Lin, C.M. Du, Y. Xiong, Appl. Catal., B 84 (2008) 468–473.
[4] K.A. Sashkina, V.S. Labko, N.A. Rudina, V.N. Parmon, E.V. Parkhomchuk, J. Catal. 299 (2013) 44–52.
[5] W. Wang, M.H. Zhou, Q.O. Mao, J.J. Yue, X. Wang, Catal. Commun. 11 (2010) 937–941.
[6] J.X. Chen, L.Z. Zhu, J. Hazard. Mater. 185 (2011) 1477–1481.
[7] Q.Q. Chen, P.X. Wu, Z. Dang, N.W. Zhu, P. Li, J.H. Wu, X.D. Wang, Sep. Purif. Technol. 71 (2010) 315–323.
[8] A. Gajovic, A.M.T. Silva, R.A. Segundo, S. Sturm, B. Jancar, M. Ceh, Appl. Catal., B 103 (2011) 351–361.
[9] T. Zhou, X.H. Wu, Y.R. Zhang, J.F. Li, T.T. Lim, Appl. Catal., B 136 (2013) 294–301.
[10] R.C.C. Costa, M. de Fatima, F. Lelis, L.C.A. Oliveira, J.D. Fabris, J.D. Ardisson, R.R.V.A. Rios, C.N. Silva, R.M. Lago, Catal. Commun. 4 (2003) 525–529.
[11] R.C.C. Costa, M.F.F. Lelis, L.C.A. Oliveira, J.D. Fabris, J.D. Ardisson, R.R.V.A. Rios, C.N. Silva, R.M. Lago, J. Hazard. Mater. 129 (2006) 171–178.
[12] F. Magalhaes, M.C. Pereira, S.E.C. Botrel, J.D. Fabris, W.A. Macedo, R. Mendonca, R.M. Lago, L.C.A. Oliveira, Appl. Catal., A 332 (2007) 115–123.
[13] R.G. Zepp, B.C. Faust, J. Hoigne, Environ. Sci. Technol. 26 (1992) 313–319.
[14] C. Tai, J.-F. Peng, J.-F. Liu, G.-B. Jiang, H. Zou, Anal. Chim. Acta 527 (2004) 73–80.
[15] B.R. Petigara, N.V. Blough, A.C. Mignerey, Environ. Sci. Technol. 36 (2002) 639–645.
[16] W.P. Kwan, B.M. Voelker, Environ. Sci. Technol. 37 (2003) 1150–1158.
[17] R.J. Watts, M.D. Udell, S.H. Kong, S.W. Leung, Environ. Eng. Sci. 16 (1999) 93–103.
[18] L. Menini, M.C. Pereira, L.A. Parreira, J.D. Fabris, E.V. Gusevskaya, J. Catal. 254 (2008) 355–364.
[19] X.L. Liang, Y.H. Zhong, H.P. He, P. Yuan, J.X. Zhu, S.Y. Zhu, Z. Jiang, Chem. Eng. J. 191 (2012) 177–184.
[20] X.L. Liang, S.Y. Zhu, Y.H. Zhong, J.X. Zhu, P. Yuan, H.P. He, J. Zhang, Appl. Catal., B 97 (2010) 151–159.
[21] S.J. Yang, H.P. He, D.Q. Wu, D. Chen, X.L. Liang, Z.H. Qin, M.D. Fan, J.X. Zhu, P. Yuan, Appl. Catal., B 89 (2009) 527–535.
[22] X.L. Liang, Y.H. Zhong, S.Y. Zhu, L.Y. Ma, P. Yuan, J.X. Zhu, H.P. He, Z. Jiang, J. Hazard. Mater. 199 (2012) 247–254.
[23] Y.H. Zhong, X.L. Liang, W. Tan, Y. Zhong, H.P. He, J.X. Zhu, P. Yuan, Z. Jiang, J. Mol. Catal. A: Chem. 372 (2013) 29–34.
[24] Y.H. Zhong, X.L. Liang, Y. Zhong, J.X. Zhu, S.Y. Zhu, P. Yuan, H.P. He, J. Zhang, Water Res. 46 (2012) 4633–4644.
[25] X.L. Liang, Y.H. Zhong, S.Y. Zhu, H.P. He, P. Yuan, J.X. Zhu, Z. Jiang, Solid State Sci. 15 (2013) 115–122.
[26] M.T. Oliva-Teles, P. Paiga, C.M. Delerue-Matos, M.C.M. Alvim-Ferraz, Anal. Chim. Acta 467 (2002) 97–103.
[27] C.F. Babbs, M.G. Steiner, Methods Enzymol. 186 (1990) 137–147.
[28] H. Zegota, J. Chromatogr. A 863 (1999) 227–233.
[29] C.J.F.t. Braak, Adv. Ecol. Res. 18 (1988) 271–317.

[30] J. Lepš, P. Šmilauer, Multivariate Analysis of Ecological Data Using CANOCO, Cambridge University Press, Cambridge, 2003.
[31] S.S. Lin, M.D. Gurol, Environ. Sci. Technol. 32 (1998) 1417–1423.
[32] V. Augugliaro, M. Litter, L. Palmisano, J. Soria, J. Photochem. Photobiol., C 7 (2006) 127–144.
[33] M. Anpo, M. Che, B. Fubini, E. Garrone, E. Giamello, M.C. Paganini, Top. Catal. 8 (1999) 189–198.
[34] H.M. Liu, W.S. Yang, Y. Ma, Y. Cao, J.N. Yao, J. Zhang, T.D. Hu, Langmuir 19 (2003) 3001–3005.
[35] M.N. Chong, B. Jin, C.W.K. Chow, C. Saint, Water Res. 44 (2010) 2997–3027.
[36] J.H. Ramirez, F.J. Maldonado-Hodar, A.F. Perez-Cadenas, C. Moreno-Castilla, C.A. Costa, L.M. Madeira, Appl. Catal., B 75 (2007) 312–323.